

The light reactions of photosynthesis*

Gernot Renger

Max-Volmer-Laboratorium für Biophysikalische Chemie, Institut für Chemie, Technische Universität Berlin, Straße des 17. Juni 135, D-10623, Berlin, Germany

This minireview summarizes our current knowledge on structure, energetics and the functional mechanisms of the reaction centres (RCs) of non-oxygenic photosynthesis and Photosystems I and II of oxygenic photosynthesis. At the RCs, the key steps of transformation of solar radiation into electrochemical free energy take place. Two types of RCs exist which differ in the nature of their electron acceptor for 'stable' light induced charge separation: iron-sulphur cluster in type I and quinone in type II. The type II of oxygenic photosynthesis is unique since it has the added machinery for oxygen evolution.

Keywords: Anoxygenic and oxygenic photosynthesis, photosystems, reaction centres.

'Hence the general struggle of life is not for resources of material and not for energy, which in form of heat, unfortunately nontransducible, plentifully exists in every organism, but it is the fight for entropy which becomes disposable through the transition from the hot sun to the cold earth. In order to make use of this transition, plants unfold unmeasurable areas of their leaves and forces the energy of the sun, in still unresolved ways, before it sinks to the temperature of the earth's surface, to carry out chemical synthesis which no one in our laboratories can even imagine.'

Ludwig Boltzmann (1844–1906)¹

BIOLOGICAL organisms are open systems far away from the thermodynamic equilibrium (about 20–25 kJ/mol)². Therefore, Gibbs free energy fluxes are required for their development and sustenance^{2,3}. [The term 'Gibbs free energy' will be used throughout this review instead of 'free energy' to characterize reactions taking place at constant pressure rather than at constant volume (Helmholtz free energy).] Electromagnetic radiation from a huge extraterrestrial nuclear power station, the Sun, is the unique source that satisfies the Gibbs free energy demand

of life on earth. The key role of solar radiation as the energetic prerequisite of the biosphere was already recognized in 1845 by Julius Robert Mayer (1814–78) and the underlying thermodynamic principle correctly formulated by Ludwig Boltzmann in 1886 (ref. 1).

Among the living organisms, two types exist that differ from the others with respect to their mode of exploitation of solar radiation as Gibbs free energy source: (i) photoautotrophs that are able to use the solar energy directly as driving force through the process of photosynthesis and (ii) photoheterotrophs that cannot perform this process and therefore need the uptake of 'energy rich' substances (food) eventually synthesized by photoautotrophs, to extract Gibbs free energy through metabolic digestion via fermentation or aerobic respiration.

The annual energy input from the Sun on our Earth is estimated to be about $5 \cdot 10^{21}$ kJ. Nearly half of this falls on the oceans and the land, about two times more on the oceans⁴. The other half is reflected by the atmosphere or absorbed by it (giving rise to storms and water movement in the oceans), only a very small fraction of less than 0.1% is eventually transformed via photosynthesis into chemical Gibbs free energy. In the overall balance, the Earth releases energy as black body radiation in the far infrared region (the maximum of the wavelength distribution is at about 10 μm) thus keeping the average temperature virtually constant.

According to van Niel, the transformation of solar radiation into Gibbs free energy can be described by the equation⁵



where H_2D and A are suitable hydrogen donor and acceptor molecules respectively. In anoxygenic photosynthesis, this process is driven by a single type of light reaction (see section on 'General structural organization of antenna and reaction centres') and H_2D s are simple molecules like H_2S or acetate (for reviews on anoxygenic photosynthesis, see refs 6–8). The bioenergetic 'big bang' in the evolution of the biosphere was the development of a system which enables the use of water as hydrogen donor concomitant with the release of O_2 and as a consequence the formation of the present day aerobic atmosphere (for reviews, see refs 9–11). This oxygen evolving (oxygenic) photosynthesis is energetically driven by two light reactions which operate in series^{12,13}.

*This is the third article on the theme 'Photosynthesis and the Global Issues' being guest-edited by Govindjee, George C. Papageorgiou and Baishnab C. Tripathy. The first article by Lars Olof Björn and Govindjee discussed the evolution of photosynthesis and the chloroplasts and was published in 2009 (vol. 96, pp. 1466–1474); the second article, by Maria Ghirardi and Prasanna Mohanty, discussed hydrogen production by algae, and was published in 2010 (vol. 98, pp. 499–507).
e-mail: gernot.renger@mailbox.tu-berlin.de

This minireview focuses on the structure and function of the reaction centres (RCs), where electronically excited singlet states populated by light absorption are directly transformed into electrochemical Gibbs free energy within the photosynthetic apparatus.

Major pigment classes participating in light reactions

Pigment molecules are indispensable constituents of the photosynthetic apparatus, especially of the RCs.

Essentially three classes of chromophores are used for this purpose: (i) (bacterio) chlorophylls with a conjugated cyclic π -electron system of (bacterio) chlorin rings, (ii) phycobilins with an open chain tetrapyrrole and (iii) carotenoids with a mainly linear chain of conjugated double bonds. Representative molecules of these pigment classes are shown in Figure 1 (for reviews, see refs 14 and 15). The photophysical properties of these pigments and their suitable interactions are affected by incorporation into a unique biopolymer material: the proteins.

The great variability of proteins in establishing controlled potential energy surfaces permits a precise tuning of the energetics of cofactors and their reaction coordinates. The availability of this 'ideal' material has enabled biological systems during a long lasting process of evolutionary development, to achieve practically any degree of specificity, efficiency and regulatory control that is required for a particular biological function.

Transformation of solar radiation into electrochemical free energy: basic principles

A landmark in our understanding of the functional pigment organization is the classical experiment, in 1932, by Emerson and Arnold¹⁶ which revealed that only one oxygen molecule is evolved per about 2500 chlorophylls when a cell suspension of a green alga *Chlorella* is illuminated with repetitive short flashes (about 10 μ s) of saturating intensity ('single turnover flashes'). As a consequence, only a very small fraction of all chlorophylls in the organisms can be directly involved in the process of transformation of an electronically excited state into the primary (electro) chemical product. This experimental observation led Gaffron and Wohl¹⁷ to the conclusion that the pigments are organized in 'photosynthetic units' and functionally distinguished in performing two basically different types of reactions: the vast majority of the pigments (> 99% of the total content) is involved in light absorption and efficient transfer of the electronically excited states to a special pigment where the photochemical reaction takes place. The former type of pigments (symbolized by P_A , where A stands for antenna) forms a light harvesting (LH) device (antenna) that enhances the optical cross-section of the photochemically active pig-

ment (designated as P_{RC} , where RC stands for reaction centres) by about two orders of magnitude. Numerous studies have shown that the functional subdivision into a large number of antenna pigments P_A and a small number of photochemically active pigments P_{RC} is a general feature of all photosynthesizing organisms.

Figure 2 shows the basic principles underlying the functions of P_A and P_{RC} within the framework of a simple HOMO (highest occupied molecular orbital)/LUMO (lowest unoccupied molecular orbital) scheme of two interacting pigments P_1 and P_2 , where one molecule attains the first excited electronic singlet state ($^1P_1^*$) whereas the other stays in the ground state (P_2)¹⁸. Two possible modes of electronic interactions between pigment molecules $^1P_1^*$ and P_2 lead to quite different results: (i) radiationless excitation energy transfer (EET) or (ii) electron transfer (ET). In the former case, the electronically excited state (exciton) is transferred from one pigment molecule to another, thus representing the function of P_A . [The term 'exciton' was originally coined in solid state physics to describe electronically excited states in crystals. In photosynthesis research, the 'exciton' is often used to describe an excited electronic state that resides during its lifetime on more than one pigment in a group of molecules¹⁹.] The EET is the underlying principle of the antenna function. Antennas are formed by ordered arrays of pigment molecules. Depending on the mode of electronic coupling between the pigments, i.e. Coulomb or exchange interaction, two different EET mechanisms emerge (Förster and Dexter type, respectively, see the next section). These EET reactions are not coupled with a net charge transfer between the interacting pigments. In marked contrast, the ET reaction leads to the formation of ion radical pair $P_1^+P_2^-$ and therefore the electronically

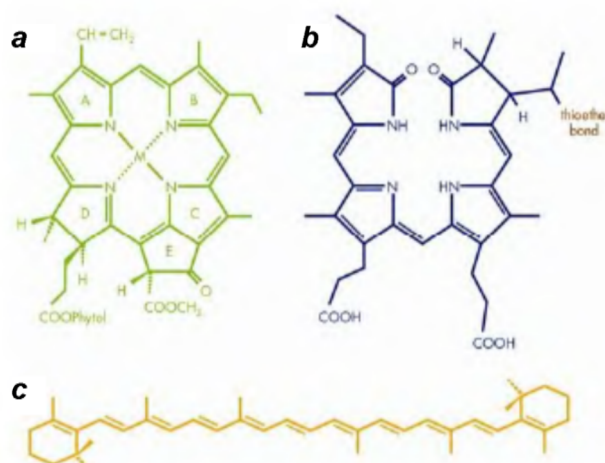


Figure 1. Chemical structure of chlorophyll *a* (a), phycocyanobilin (b) and all-trans- β -carotene (c) as representative species of chlorophylls, phycobilins and carotenoids. In bacteriochlorophylls, the double bond of ring B in chlorins is hydrated forming bacteriochlorins (electronic version prepared by S. Renger).

excited pigment $^1P_1^*$, which transfers an electron to P_2 as its coupled electron acceptor, reflects the photochemically active pigment P_{RC} . This type of ET is the key step in the overall transformation process of solar radiation into (electro) chemical Gibbs free energy through the process of photosynthesis. The mechanism of ET reactions can be described within the framework of the Marcus theory (for details, see the next section).

Theoretical background on excitation energy and electron transfer

Figure 3 illustrates schematically the two types of interactions that determine the properties of pigment–protein complexes: (i) pigment–pigment and (ii) pigment–protein coupling. The strength of these couplings determines the mechanistic details of EET and ET in pigment–protein complexes. The theoretical background of these processes

has been described in a recent review²⁰ and a book chapter²¹ and therefore the theoretical background of EET and ET is briefly summarized and only few widely used formulas are presented here.

Excitation energy transfer

In the weak coupling case, the electronically excited state (exciton) hops during its lifetime stepwise from one pigment to a neighbour within the antenna complex. In this case, the EET rate between two pigments can be described by the formula of Förster²².

$$k_{EET}^{DA} = \frac{R_0^6}{\tau_0} \cdot \frac{1}{R^6} \quad (2a)$$

with τ_0 = intrinsic lifetime of the donor emission and

$$R_0^6 = \frac{A\kappa^2}{n^4} \int F_D(\nu) \epsilon_A(\nu) \frac{d\nu}{\nu^4}, \quad (2b)$$

where R is the distance between the transition dipole moments of the donor and acceptor pigment, A a constant, κ a factor that describes the mutual orientation of the transition dipole moments, n the refractive index of the medium, $F_D(\nu)$ and $\epsilon_A(\nu)$ are the spectral distributions of the normalized donor emission and of the acceptor absorption, respectively.

The Förster mechanism is based on classical Coulomb interactions and on the approximation of point dipoles. In spite of its limitations, the expression of Förster resonance energy transfer (FRET) is widely used for data interpretation in biological systems (for a review, see ref. 23).

The pigment protein interaction affects the shape of $F_D(\nu)$ and $\epsilon_A(\nu)$ and therefore modulates the EET rate.

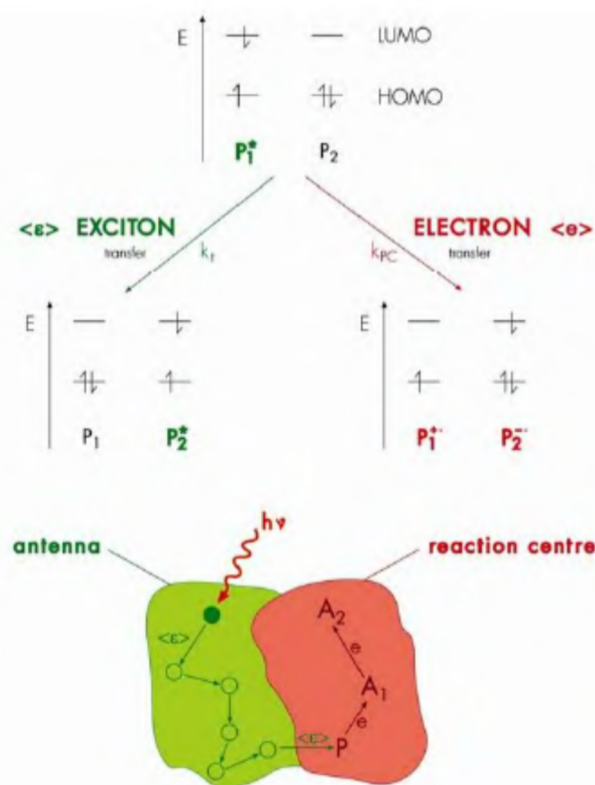


Figure 2. Electronic coupling between two pigment molecules (P_1 and P_2) with the same orbital structure. One pigment is in the first excited electronic singlet state ($^1P_1^*$) and the other in the electronic ground state (P_2); HOMO and LUMO = highest occupied and lowest unoccupied molecular orbital respectively. The top part illustrates the processes of excitation energy transfer (EET) (green symbols) and electron transfer (ET) (red symbols) whereas the lower part shows a schematic representation of an antenna (in green) and reaction centre (in red) complex, $\langle e \rangle$ and $\langle e^- \rangle$ symbolize an exciton and electron respectively, and k_t and k_{PC} are the rate constants of EET and ET respectively. P represents the photoactive pigment and A_1/A_2 electron acceptor components (electronic version prepared by S. Renger).

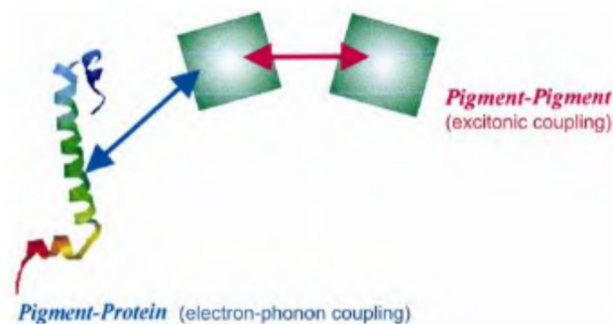


Figure 3. A scheme of pigment–pigment and pigment–protein interactions (symbolized by red and blue arrows respectively) in pigment–protein complexes. Pigments are represented by green squares and the protein by an α -helix (electronic version prepared by P. Kühn). See text for details.

An important effect emerges when the electronic wave functions of the donor and acceptor pigment significantly overlap at sufficiently short distances. In this case, non-classical quantum mechanical exchange takes place which gives rise to a mechanism, which is designated as Dexter type EET²⁴. The rate constant of this EET depends on the electronic matrix element of the exchange coupling and the overlap integral $\int F_D(\nu) \epsilon_A(\nu) d\nu$.

The Dexter mechanism is important for photosynthetic organisms because it permits – according to the spin selection rules – the quenching of (B)Chl triplets by carotenoids (Cars) in its singlet ground state (for a detailed explanation, see ref. 25). The process $^3(\text{B})\text{Chl} + ^1\text{Car} \rightarrow ^1(\text{B})\text{Chl} + ^3\text{Car}$ followed by radiationless decay of ^3Car is indispensable for protection of the apparatus to photodynamic destruction under aerobic conditions (for a review, see ref. 26). This protection cannot occur via a Förster-type EET because it is ‘spin-forbidden’ (see ref. 25). Therefore (B)Chls and Cars have to be in close enough contact to permit an efficient Dexter type triplet transfer to Cars. The rate of the transfer from $^3(\text{B})\text{Chl}$ to ^1Car can be significantly faster than ^3Chl formation by intersystem crossing, as illustrated for the antenna complex LHC II²⁷ of green plants.

In the case of strong pigment–pigment interaction, the excited state is delocalized over the ensemble and a ladder of exciton states emerges concomitant with a redistribution of the oscillator strength (see refs 20 and 21 and references therein). A rapid coherent oscillation of the excitation among the pigment ensemble takes place if phase correlation exists. However, this phase relation disappears within <1 ps at room temperature due to interaction with the environment. In spite of this rather short time domain, the coherent EET appears to play an important role for the efficiency of light harvesting by the antenna complexes in photosynthesis (see ref. 28 and references therein).

If the pigment–protein interaction is weak, the relaxation between exciton states can be modelled by the Redfield theory which describes the coupling of a multilevel system of excited states with the environment. A more complex pattern arises when both pigment–pigment and pigment–protein couplings are strong. In this case, a modified Redfield theory can be used (for further information, see refs 20, 21 and 28).

In large pigment–protein complexes like the core complexes of photosystem I (see section on ‘Photosystem I’) and photosystem II (see section on ‘Photosystem II’), some pigments are strongly coupled forming domains which are connected via Förster type EET. In these complexes, a generalized Förster theory must be used to describe the EET between an exciton state of domain i with an exciton state j , whereas the exciton relaxation within each domain is dealt with by Redfield or modified Redfield theory (for details, see references in refs 20 and 28).

Electron transfer

Electron transfer (ET) reactions in biological systems take place via vibrationally coupled electron tunnelling (for review, see refs 29 and 30). In a first order approximation, the rate constant of an ET from donor D to acceptor A can be calculated by evaluating the relation (‘Golden Rule’)

$$k_{\text{ET}}^{\text{DA}} = \frac{2\pi}{\hbar} |V_{\text{DA}}|^2 \text{FCWD}, \quad (3)$$

where $\hbar = h/2\pi$ (h = Planck constant), V_{DA} is the matrix element of electronic coupling and FCWD the Franck–Condon weighted density of states.

At weak electronic coupling the ET is nonadiabatic. A classical treatment of the vibrations in the Franck–Condon factor leads to the widely used Marcus formula for nonadiabatic electron transfer (NET)

$$k_{\text{NET}}^{\text{DA}} = \frac{2\pi}{\hbar} |V_{\text{DA}}|^2 (4\pi\lambda k_{\text{B}}T)^{-1/2} \times \exp[-(\Delta G_{\text{DA}}^0 + \lambda)^2 / 4\lambda k_{\text{B}}T], \quad (4)$$

where ΔG_{DA}^0 is the standard Gibbs free energy gap between states $\text{D}^{\text{red}}\text{A}^{\text{ox}}$ and $\text{D}^{\text{ox}}\text{A}^{\text{red}}$, λ the reorganization energy and k_{B} the Boltzmann constant. The Marcus theory on ET reactions by vibrationally coupled electron tunnelling is of fundamental relevance for understanding the mechanism of redox reactions; for this work, Marcus was awarded the Nobel Prize in Chemistry in 1992.

The matrix element V_{DA} depends on the overlap between the electronic wave functions and therefore decreases exponentially with edge-to-edge distance (R_{DA}) between components D and A. This dependence is the basis for the empirical ‘Dutton-rule’ providing a simple relation between the rate constant $k_{\text{NET}}^{\text{DA}}$ and the parameters ΔG_{DA}^0 , λ and R_{DA} of NET steps in biological systems³¹. Insertion of the relation $|V(R_{\text{DA}})|^2 = |V(R_{\text{DA}} = 0)|^2 \exp(-\beta R_{\text{DA}})$ into eq. (4) and using a value of $\beta = 1.4 \text{ (\AA)}^{-1}$ leads, after suitable algebraic rearrangement, to eq. (5).

$$\log k_{\text{NET}}^{\text{DA}} = 15 - 0.6R_{\text{DA}} - 3.1(\Delta G_{\text{DA}}^0 + \lambda)^2 / 4\lambda. \quad (5)$$

The algebraic form of eq. (5) is only valid if the physical parameters are used in units of s^{-1} ($k_{\text{NET}}^{\text{DA}}$), \AA (R_{DA}) and eV (ΔG_{DA}^0 and λ). The above value of β was shown to be appropriate for many biological systems (in fact β can vary depending on the packing density of the protein matrix; for further details, see refs 21 and 33).

Equations (4) and (5) show that the ET rate depends on ΔG_{DA}^0 , λ and R_{DA} and that modulation of the distance between D and A provides the most powerful tool to vary kinetics over wide ranges (orders of magnitude). The

'Dutton-rule' which has been refined by considering the packing density of atoms between D and A is a useful starting point for estimations of ET rates in photosynthesis and respiration^{31,32}. For further reading on more detailed models, see ref. 33 and references therein.

Energetics of photosynthetic solar energy transformation

The RCs can be considered as nanoscale machines which transform the energy of a photon flux into the current of electrochemical work.

For the limiting case of full reversibility, the maximum efficiency η_{\max}^{RC} of RC can be calculated within the framework of a classical 'Carnot type machine', where a flux of heat energy from higher to lower temperature level is transformed into useful work (for details, see textbooks of *Physical Chemistry*, e.g. ref. 34). The value of η_{\max}^{RC} is given by

$$\eta_{\max}^{\text{RC}} = (T_{\text{solar}} - T)/T_{\text{solar}}, \quad (6)$$

where T_{solar} is the 'effective temperature' of the scattered nonpolarized solar radiation impinging on RC and T its ambient temperature. RC is assumed to be a 'narrow band absorber' which uses nearly monochromatic red light at a wavelength $\lambda(\text{RC})$ which corresponds to the absorption maximum of chlorophyll *a* (Chl *a*). A number of about 73% was obtained³⁵ for $\eta_{\max}^{\lambda(\text{RC})}$ by using a calculated value of about 1100 K for T_{solar} (refs 35 and 36) and a wavelength of 680 nm for $\lambda(\text{RC})$.

The overall maximum efficiency η_{\max} drops down when we take into account the whole spectrum of solar radiation and a threshold wavelength $\lambda(\text{RC})$ of 700 nm for the photons that can be transformed into electrochemical Gibbs free energy while the excess energy of shorter wavelength photons is lost as heat. The value of η_{\max} is obtained according to the relation

$$\eta_{\max} = \eta_{\max}^{\lambda(\text{RC})} \cdot 1.77 \cdot \int_0^{\lambda(\text{RC})} \rho(\lambda) d\lambda \bigg/ \int_0^{\infty} \frac{hc}{\lambda} \rho(\lambda) d\lambda, \quad (7)$$

where $\rho(\lambda)$, h and c are the photon flux density of solar radiation impinging the earth surface at wavelength λ , the Planck constant and the velocity of light in vacuum, respectively, and 1.77 is the energy of a photon at 700 nm in units of eV.

The application of eq. (7) leads to a value of about 30% for η_{\max} (ref. 36).

Equation (7) reveals that the magnitude of η_{\max} depends on $\lambda(\text{RC})$. Therefore, it is interesting to consider the possibility that during evolution a $\lambda(\text{RC})$ could have been selected for achieving the optimum of η_{\max} . This idea, however, cannot be tested in a straightforward manner (for a recent analysis, see ref. 37).

It must be emphasized that the maximum efficiency of a reversible system is only achieved if no Gibbs free energy is used for driving any process at a finite, i.e. a physiological, rate. The efficiency of an energy converter acting as a thermodynamically open system which couples energy fluxes and forces is described by the rules of irreversible thermodynamics. Details of these calculations are beyond the scope of this review (for further information, see ref. 38). A value of about 20% was estimated for the maximum efficiency of solar energy conversion in the RCs of green plants and algae when considering realistic rate constants for the forward and the back reactions³⁹. RCs drive the electron transport chain and photophosphorylation which leads to further energy losses so that eventually a maximum efficiency of about 5% is obtained for oxygenic photosynthesis. This number fits with experimental data on rapidly growing 'cultures' like sugarcane under optimal conditions.

At first glance, the overall efficiency of a few per cent for photosynthesis seems to be surprisingly low when considering the long selection pressure during evolution and comparing it with devices like photovoltaic cells. However a direct comparison with the latter systems is highly misleading because the energetics of photosynthetic organisms comprises all costs for synthesis and repair of the apparatus. Therefore, these energy costs must be taken into account to obtain meaningful numbers.

With respect to thermodynamic considerations on photosynthesis, another point must be mentioned. Some time ago, photosynthetic RCs were erroneously suggested not to follow the second law of thermodynamics⁴⁰. It is clear that this is not the case⁴¹. Further, the described type of calculation on the efficiency of photosynthesis as energy converter of solar radiation must not be confused with estimates on the fraction of the photon energy that is transformed into a particular radical pair on individual RCs⁴². Estimates of these number are given in the sections on 'different RCs and photosystems'.

General structural organization of antenna and reaction centres

Figure 2 raises questions on the nature and structure of the devices that were assembled during a long evolutionary process to perform these reactions in the photosynthetic apparatus with high efficiency and in a controlled manner.

The antenna systems are pigment-protein complexes which provide optimal adaptation to different illumination conditions in space (location area) and time (diurnal and seasonal changes). Therefore a great variety of arrays exists among anoxygenic bacteria, oxygen evolving cyanobacteria, algae and plants. Figure 4 presents characteristic examples. The top panel shows a general structure of the antenna system of anoxygenic purple bacteria and

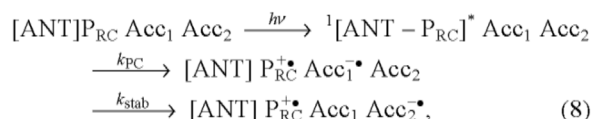
EET pathways⁴³. These integral pigment–protein complexes are characterized by a circular array of the BChls. The bottom panel schematically illustrates the quite different structures of the antenna systems in oxygen evolving cyanobacteria and red algae (left side) and plants (right panel). For details on antenna systems, see refs 44 and 45.

In marked contrast to the flexibility of antenna systems, RCs are rather invariant to evolutionary development with one great exception, i.e. the ‘invention’ of a ‘molecular machine’ for oxidative water splitting as the indispensable step up to the level of oxygen evolving photosynthetic organisms (vide infra).

Two types of RCs exist, designated type I and type II (see the next section). In anoxygenic photosynthesis, RCs are structurally separated operational units but in oxygenic photosynthesis, they are integral parts of larger complexes, referred to as photosystem I (PS I) and photosystem II (PS II). Furthermore, the RCs in different anoxygenic bacteria act as single ‘solar power stations’ in driving the photosynthetic electron transport whereas PS I and PS II cooperate in series^{12,13} to perform NADP⁺ reduction with water as hydrogen donor, thus leading to concomitant O₂ release. Apart from these distinct modes of operation, the photosystems differ from

the RCs of anoxygenic photosynthetic bacteria by: (i) significantly larger number of subunits, (ii) binding of core antenna pigments and (iii) in the case of PS II, the presence of the water oxidizing complex (WOC) as an integral constituent.

Regardless of structural and functional differences between type I and type II RCs and PS I and PS II, the mechanism of the light-induced charge separation is basically the same that is described by the general scheme of eq. (8):



where the first step summarizes the population of the lowest electronically excited singlet state ${}^1\text{P}_{\text{RC}}^*$ by light absorption and EET from pigments of the antenna [ANT] including rapid internal conversion and excitation equilibration symbolized by ${}^1[\text{ANT} - \text{P}_{\text{RC}}]^*$ (without specifying the details of the processes), k_{PC} is the rate constant of the primary charge separation step giving rise to the formation of the radical ion pair $\text{P}_{\text{RC}}^+\text{Acc}_1^-$, with Acc_1 acting as the primary electron acceptor, and k_{stab} is the rate constant for stabilization of the charge separation by rapid ET from Acc_1^- to component Acc_2 . This generalized description does not explicitly account for the participation of additional cofactors in the ET pathway from Acc_1^- to Acc_2 . Likewise, for simplicity the back reactions are omitted in eq. (8). Furthermore, in PS I and PS II two ET steps are involved on the donor side (see sections on ‘Photosystem I’ and ‘Photosystem II’).

In general, the two types of RCs differ mainly with respect to the directionality of the charge separation pathway(s) and in the chemical nature of their acceptor side cofactors, i.e. Acc_2 of type I RCs is an iron–sulphur cluster covalently linked to the protein matrix but the Acc_2 in type II RCs is a special noncovalently bound paraquinone molecule (Q_A).

Reaction centres of anoxygenic purple bacteria

Green sulphur bacteria (Chlorobiaceae) and heliobacteria (Heliobacteriaceae) contain type I RCs whereas the RCs of purple bacteria (Proteobacteriaceae) and green filamentous nonsulphur bacteria (Chloroflexaceae) are type II RCs. RCs from anoxygenic bacteria can be isolated as functionally fully competent operational units⁴⁶. This great achievement was a milestone in photosynthesis research because it provided the ideal sample material for detailed analyses of the structure and reaction pattern of RCs (see ref. 47 and references therein).

In most cases, the protein matrix which binds the cofactors for the light-induced charge separation leading

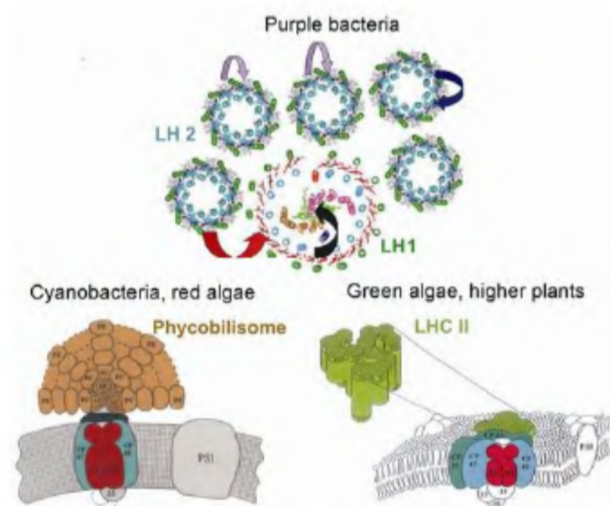


Figure 4. A schematic representation of antenna complexes in anoxygenic purple bacteria (top panel), oxygen evolving cyanobacteria and red algae (bottom panel, left side) and green plants (bottom panel, right side). The top panel represents a view of the structure perpendicular to the membrane plane and also indicates by arrows the intramolecular EET inside LH (light harvesting) 2 and intermolecular EET from LH2 to LH1 (red arrow) and from LH1 to reaction centre (RC) (black arrow). For further details, see ref. 43 (the figure was provided by R. Cogdell). The bottom panel shows on the left side, a schematic representation of the extrinsic phycobilisome antenna complex (marked in brown) attached to photosystem (PS) II and on the right side, of the main intrinsic antenna complex LHC (light harvesting complex) II (marked in green) connected with PS II (electronic version prepared by C. Theiss). For further details, see ref. 25.

to the radical pair $P_{RC}^{+\bullet} Acc_2^{\bullet}$ is a heterodimer consisting of two different polypeptides, but at least in one case (Heliobacteriaceae), it is a homodimer^{7,48}.

According to our current knowledge, the photoactive pigment P_{RC} is a special pair of two strongly excitonically coupled bacteriochlorophyll molecules in all non-oxygen evolving (anoxygenic) photosynthetic bacteria. The symbols for P_{RC} in different RCs are deduced from the peak position of the bleaching band in the near infrared (NIR) region of the oxidized minus reduced difference spectrum, e.g. P870 is the P_{RC} of the RC of *Rhodobacter (Rb.) sphaeroides* (vide infra). Different BChl molecules are used for the special pair of the photoactive pigment P_{RC} : BChl *a* and BChl *b* in all type II RCs (P870, P960) and BChl *a* in type I RCs (P840) of Chlorobiaceae and in addition BChl *g* in the type I RCs of Heliobacteriaceae (P798)⁷.

In type II RCs, the acceptor components Acc_1 and Acc_2 of eq. (8) are BChl *a* or *b* and ubiquinone or menaquinone, respectively, with bacteriopheophytin (BPheo) *a* or *b* acting as an intermediary ET component (vide infra). The primary acceptor Acc_1 of type I RCs is Chl *a* in Chlorobiaceae and a 8¹-hydroxychlorophyll *a* in Heliobacteriaceae and the component Acc_2 is an iron-sulphur cluster where a quinone (in many cases a menaquinone) with exceptionally low reduction potentials (see section on 'Photosystem I') probably mediates the ET from Acc_1 to Acc_2 , as is known for PS I (see the next section). However the information is rather fragmentary for type I RCs from anoxygenic bacteria⁷.

The quantum yield of light-induced charge separation was found to be about 1 in RCs from *Rb. sphaeroides* (formerly named *Rhodospseudomonas sphaeroides*)⁴⁹ under low photon flux densities, where ET steps are not rate limiting for the overall process.

Only a fraction of the photon energy is stored in the form of an electrochemical potential difference and this value decreases in the energetically downhill sequence of the different radical pair states that are transients in the route of light-induced charge separation of the RCs. Therefore, this fraction is a time dependent parameter related to the radical pair state under consideration. Furthermore, protein relaxation processes essentially affect the energetics (for a discussion, see ref. 50). In the following, the state of the relaxed radical pair $P^{+\bullet} Acc_2^{\bullet}$ (see eq. (8)) will be used as the reference for energetic characterization of the 'stable' charge separation in the RCs. The light-induced reaction sequence starts from the lowest excited singlet state of $^1P_{RC}$. Accordingly, a photon with minimum energy for achieving charge separation has to be in resonance with the transition into this lowest excited singlet state, i.e. the wavelength of this photon has to be 870 nm for P870. The Gibbs free energy stored in the stabilized radical is approximately given by the difference between the redox potentials of $P/P_{RC}^{+\bullet}$ and Acc_2^{\bullet}/Acc_2 because the distance of the two radicals is suffi-

ciently large so that the electrostatic interaction energy between the radical ions $P_{RC}^{+\bullet}$ and Acc_2^{\bullet} can be neglected; redox potentials are equilibrium parameters that always reflect the Gibbs free energy difference between relaxed states. The redox potential of protonatable components depends on pH due to different pK values of the oxidized and reduced form. Therefore the use of the midpoint potentials at pH = 7.0, $E_{m,7}$ is more convenient for the characterization of the energetics of biological systems rather than using standard redox potentials defined for the nonphysiological pH = 0.

The E_m values of $P_{RC}/P_{RC}^{+\bullet}$ are about +0.25 V in type I RCs and about +0.5 V (Proteobacteriaceae) and +0.35 V (Chloroflexaceae) in type II RCs⁷. Less precise information is available on E_m data for Acc_2^{\bullet}/Acc_2 . Numbers of about -0.1 V were reported for Q_A^{\bullet}/Q_A of type II RCs⁵¹, whereas the values for the iron-sulphur clusters of type I RCs are much lower (<-0.5 V, see section on 'Photosystem I').

Based on these numbers, the Gibbs free energy stored in the radical pair $P_{RC}^{+\bullet} Acc_2^{\bullet}$ is about 35–40% of a photon with an energy corresponding to that of the transition into the lowest excited singlet state $^1P_{RC}$ in type II RCs and 50–60% in type I RCs.

The type I RCs are functionally and structurally much less characterized than the type II RCs of the phylum Proteobacteriaceae. Therefore, the properties of these thoroughly analysed type II RCs will be described in more detail to illustrate the characteristics of RCs from anoxygenic photosynthetic bacteria and the typical features of type I RCs outlined in the section 'Photosystem I'.

The structure of RCs from *Blastochloris (Bl.) viridis* (formerly named *Rhodospseudomonas viridis*) was first resolved at atomic resolution by Deisenhofer *et al.*⁵². This pioneering work opened the road for a much deeper understanding of the structure and functions of photosynthetic RCs and was awarded the Nobel Prize in Chemistry in 1988.

During the last two decades, enormous progress has been achieved⁵³ and now the corresponding structure information, at atomic resolution, is also available on core complexes of PS I and PS II (see sections on 'Photosystem I' and 'Photosystem II').

The top panel of Figure 5 shows the general overall structure (Figure 5a) and the array of cofactors (Figure 5b) of type II RCs from the anoxygenic purple bacterium *Bl. viridis* (the nature of the c-type electron donor markedly varies among different species, see refs 7 and 53). Each subunit of the heterodimer (denoted L and M) forms five transmembrane helices. The cofactors (special pair P_{RC} , two monomeric BChls, two BPheos, two quinones) are arranged in two branches in a highly symmetric manner around a pseudo C2 axis crossing the nonhaeme iron (NHFe) centre (see Figure 5b). Interestingly, the light induced ET occurs via a unidirectional pathway comprising the cofactors marked by coloured symbols. This

'active' route from P_{RC} to Q_A is on the 'A-branch'. An ET through the 'inactive' pathway (B-branch) can be achieved with only much lower efficiency in RCs from specially engineered mutants⁵⁴.

The bottom panel of Figure 5 shows a simple scheme of ET steps of charge separation via the A branch. The kinetics of these reactions have been resolved in great detail by time-resolved spectroscopic techniques (for a review, see ref. 55 and references therein).

Excited singlet states populated by direct absorption of isolated RCs are transferred to P_{RC} within 100 fs. The subsequent primary charge separation takes place with a

time constant of about 3 ps followed by a rapid ET (< 1 ps) from $BChl_A^+$ to $BPheo_A$ (subscript A symbolizes cofactors of the A-branch). The 'stabilization' of the charge separation by ET from $BPheo_A^+$ (often symbolized by H_A) occurs with a time constant of about 200 ps. Interestingly, these reaction steps are slightly faster at lower temperatures⁵⁶. This finding indicates that the protein flexibility does not affect the formation of the stable ion radical pair $P^+ \cdot Q_A^-$. In marked contrast, the reoxidation of Q_A^- by Q_B is strongly temperature dependent and requires a flexible protein matrix^{57,58}. This feature appears to be a general phenomenon of type II RCs (see also section on 'Photosystem II').

Photosystem I

Photosystem I (PS I) contains a type I RC that has been thoroughly analysed; it nicely reflects the general characteristics of type I RCs (for review articles, see chapters in ref. 59).

The structure of trimeric PS I complexes from the thermophilic cyanobacterium *Thermosynechococcus* (*T.*) *elongatus* was resolved at atomic resolution by Fromme, Witt, Saenger and coworkers⁶⁰. Recently, the structure of PS I from higher plants has been obtained by Nelson and coworkers⁶¹.

The top panel of Figure 6 shows structure and cofactor arrangement of PS I from *T. elongatus*⁶². The cofactors of the RCs are bound to a heterodimeric protein matrix consisting of polypeptides PsaA and PsaB, each forming 11 transmembrane helices. The cofactors are symmetrically arranged in two branches around a pseudo C2 axis (Figure 6d, top panel) like in RCs of anoxygenic bacteria (type I and type II). A special pair type structure motif formed by one Chl *a* and one Chl *a'* (the epimer of Chl *a* at the C13 position) resembling the special pair P in RCs of anoxygenic bacteria was assigned to be the photoactive pigment P_{RC} of PS I, designated P700 (see Bessel Kok⁶³ for its discovery). However, this idea on the functional role of P700 has to be somewhat modified (vide infra). Acceptor Acc_1 is also Chl *a* symbolized by A_0 and Acc_2 is an iron-sulphur cluster F_X located at the symmetry axis (see Figure 6d, top panel) and coordinated by both subunits PsaA and PsaB. Two possible parallel pathways exist for ET from P700 to F_X including four Chl *a* and two phylloquinone molecules symbolized by A_{1A} and A_{1B} . These two quinone molecules are characterized by unusually low midpoint potentials due to tuning of the properties of these cofactors by the protein matrix^{64,65}. We now know that – in marked contrast to the unidirectional pathway in type II RCs (see earlier section) and PS II (see the next section) – the charge separation leading to the formation of the radical pair $P700^+ \cdot F_X^-$ comprises a bidirectional electron transport chain, with different efficiencies of the A- and B-branches. The extent of this branching probably varies among different species and

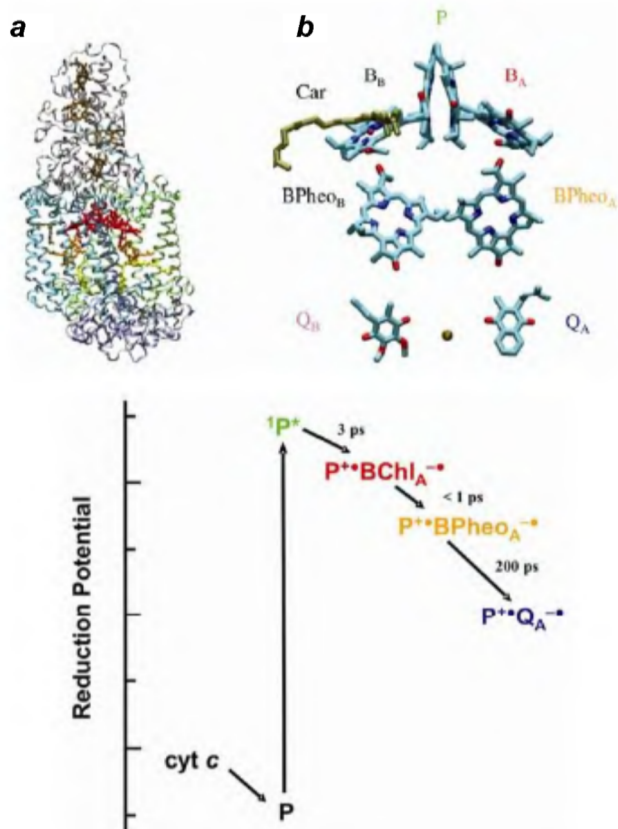


Figure 5. Structure and cofactor arrangement of RC from purple bacterium *Blastochloris* (*Bl.*) *viridis* (top panel) and reaction pattern (bottom panel) (data provided by W. W. Parson). Top panel: (a) Crystal structure, the L, M, H and C subunits are represented as ribbons in green, cyan, ice-blue and silver, respectively; the four BChls and two BPheos are shown in red and orange, respectively; menaquinone (Q_A) and ubiquinone (Q_B) are in yellow; the hemes and nonheme iron atom are in ochre; and the carotenoid (dihydroneurosporene) is in tan (b) cofactors: the BChls (P, B_A and B_B), BPheos, quinones (Q_A and Q_B), non-heme Fe atom (ochre sphere), and carotenoid (car), the side chains of the BChls, BPheos and quinones are truncated, cofactors of the active A-branch and the inactive B-branch are characterized by coloured and black symbols respectively. Bottom panel: A simplified scheme of the energetics of $P^+ \cdot Q_A^-$ formation via the A-branch. Symbols denote: P^* = excited singlet state of P; P^+ = cation radical of P, $BChl_A^+$, $BPheo_A^+$ and Q_A^+ = anion radicals of $BChl_A$, $BChl_B$ and Q_A , respectively. The energy scale is not linear, the energy gaps between P^* and $P^+ \cdot BChl_A^-$ and between $P^+ \cdot BChl_A^-$ and $P^+ \cdot BPheo_A^-$ are much smaller than the gap between $P^+ \cdot BPheo_A^-$ and $P^+ \cdot Q_A^-$. See text for details.

under different conditions; its physiological role is not yet clear^{64,66}.

In addition to the cofactors for the light-induced charge separation, the PsaA/PsaB heterodimer also binds antenna pigments (the total pigment content comprises 96 Chl and 22 Car molecules⁶²).

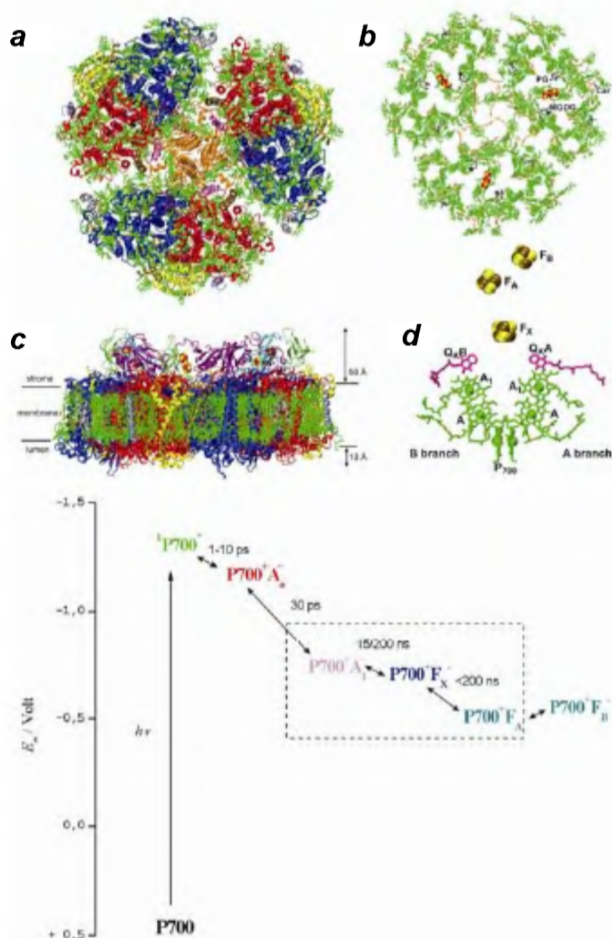


Figure 6. Structure and cofactor arrangement (top panel, data provided by P. Fromme and I. Grotjohann) and reaction pattern (bottom panel, data provided by P. Setif) of PS (photosystem) I. Top panel: (a) View of the trimer from the luminal side; (b) View along the membrane plane. All extrinsic subunits of PS I are found on the cytoplasmic/stromal side, where the protein complex extends almost 50 Å out of the membrane, whereas loops reach maximally 10 Å into the lumen; (c) Non-protein cofactors: chlorophylls and carotenoids are marked in green and brown respectively. Two lipids in the vicinity of F_X and the phytylquinones are also shown, with one side having a neutral lipid (MGDG = monogalactosyldiacylglycerol), whereas the other side contains the charged lipid PG (phosphatidylglycerol) which might have functional implications, carotenoids Car 14 and Car 17 are close enough to play a protecting role for the chlorophyll cofactors involved in light-induced charge separation; (d) Cofactors of the electron transfer chain: chlorophylls and phytylquinones are marked in green and magenta respectively. Bottom panel: A simplified scheme of the energetics of $P700^+ F_X^-$ formation and subsequent ET to $F_{A,B}$. Symbols represent: $^1P700^+$ and $P700^{++}$ the lowest excited singlet state and cation radical, respectively, of P700; A_0^- and A_i^- the anion radicals of acceptors Chl *a* and phytylquinone respectively; F_X , F_A and F_B the iron sulphur centres. See text for details.

The whole PS I complex contains 12 subunits. Three subunits (PsaC, D and E), which do not form transmembrane helices, are attached to the complex on the cytoplasmic side (in plant chloroplasts, the stroma side) as is shown in Figure 6d, top panel. Among these three subunits, only PsaC binds cofactors, i.e. the two iron–sulphur clusters F_A and F_B (Fe_4S_4 -type) which are reduced by F_X^- (see Figure 6, bottom panel).

The other subunits, which form at least one transmembrane helix, are mainly responsible for stabilization of the PS I complex⁶². The nature of these subunits slightly differs between cyanobacteria and plants^{61,62}.

The light-induced charge separation in PS I comprises ET through both branches although the A-branch seems to be favoured in most cases^{64,66}. The variability in using the two pathways under different conditions does not permit the presentation of a generalized detailed scheme for the kinetics of the ET steps through both the branches. Therefore, only an overall scheme of individual redox steps of the sequence $P700 \rightarrow A_0 \rightarrow A_i \rightarrow F_X \rightarrow F_{A,B}$ is presented, as shown in the bottom panel of Figure 6. The first detectable radical pair $P700^+ \cdot A_0^-$ is formed in a few picoseconds. This reaction comprises the participation of two Chl *a* molecules in each branch. Contrary to the earlier idea of $^1P700^*$ acting as primary electron donor, the monomeric Chl *a* located between P700 and A_0 (see Figure 6d) was inferred to take this function⁶⁷ thus initially leading to the formation of the radical pair Chl *a* $^+ \cdot A_0^-$ followed by rapid ET from P700 to Chl *a* $^+$ (for simplicity, no distinction is made between the two branches). This idea has been supported by a recent study on mutants from the green alga *C. reinhardtii*⁶⁸. The reduced components A_{0A}^- and A_{0B}^- are reoxidized by phytylquinones A_{1A} and A_{1B} in the time domain of tens of picoseconds. These kinetics are about one order of magnitude faster than those of $BPheo_A^-$ reoxidation by Q_A in type II RCs. The reoxidation of $(A_{1A}, A_{1B})^-$ by F_X occurs in the nanosecond time domain with biphasic kinetics which may reflect the transfer steps in the PsaB (slow kinetics) and PsaA branch (fast kinetics). Since the ET from F_X^- to F_A (F_B) is faster than F_X^- formation and due to possible involvement of reversibility, it is difficult to resolve individual kinetic steps and assignment is model dependent (for details, see refs 64 and 65).

The minimum energy of a photon which enables an electronic transition at 700 nm is 1.77 eV. Values of +420 to +470 mV have been reported for the midpoint potentials of $P700/P700^+$ from different organisms (see references in ref. 64). Uncertainties exist in the determination of E_m for F_X ; numbers in the range of –540 to –640 mV seem to be most reliable⁶⁹. Based on these data a fraction of 55–65% of the photon energy is calculated to be maximally ‘stored’ in the state $P700^+ \cdot F_X^-$. When relating to the reduced F_A/F_B centres, this value drops down to 50–55%.

Photosystem II

The photosystem II (PS II) complex is unique because of its capability to split water with solar radiation into metabolically bound hydrogen and O₂. This system, which contains a type II RC, acts as water:plastoquinone-oxido:reductase (for reviews on different facets of PS II, see ref. 70). The essential reactions of the overall process are those of the oxidative water splitting. Two key evolutionary steps were required to transform a type II RC into a 'water splitting machine': (i) tuning of the properties of photoactive pigment P_{RC} to generate a strongly oxidizing cation radical P_{RC}⁺ as the indispensable driving force for the eventual electron abstraction from water and (ii) 'invention' and assembly of a catalytic device which enables the energetic tuning of a redox process involving the cooperation of four strongly oxidizing redox equivalents to split water into O₂ and four protons.

It must be emphasized that the former goal was not achieved by cofactor replacement (BChl *a* → Chl *a*) but by evolutionary engineering of the protein environment^{71,72}. This finding is another striking example for illustrating the potential of proteins in tuning the properties of cofactors. In the case of PS II, the *E_m* value of Chl *a*/Chl *a*⁺ is drastically increased from about +0.8 V in solution⁷³ to about +1.25 V (ref. 74) of the photoactive Chl *a* complex designated P680⁺, whereas in PS I, the modulation by the environment leads to an *E_m* shift in the opposite direction, i.e. to values below +0.5 V (ref. 64) for P700/P700⁺. However, a replacement of BChl by Chl was required for energetic reasons to populate a lowest excited singlet state with high enough energy to permit formation of a sufficiently stable radical pair P680⁺ Q_A[•].

The P680⁺ cation radical of PS II is one of the most oxidizing species within biological systems. In analogy to the special pair P in RCs of anoxygenic bacteria and P700 of PS I, the photoactive pigment of PS II has been symbolized by P680 according to its characteristic red bleaching band in the difference spectrum of photo-oxidation (for details, see ref. 75). However, for a more specific description it is most important to keep in mind that – due to the excitonic coupling of six pigments⁷⁵ – the situation in PS II is more complex than in type II RCs of anoxygenic bacteria, where the states ¹P*, ³P and P⁺ are all localized on the 'special pair' P. As a striking difference, in PS II the lowest excited singlet state ¹P680* is the lowest exciton state of the electronically excited pigment complex ¹(P_{D1}P_{D2}Chl_{D1}Chl_{D2}Pheo_{D1}Pheo_{D2})* (with the largest contribution from the eigenstate of ¹Chl_{D1}, see refs 75 and 76) rather than ¹(P_{D1}–P_{D2})*. The energetic gaps between the exciton levels are so small that at room temperature the excited singlet state is distributed over all the six pigments with population probabilities of each pigment ranging from 10% to 30% (see ref. 75). The triplet state ³P680 represents ³Chl_{D1} but not ³(P_{D1}–P_{D2}) and

the primary cation radical P680⁺ is Chl_{D1}⁺ rather than (P_{D1}–P_{D2})⁺ which is formed via a secondary ET step. Therefore, the symbol P680 should be used with caution by keeping in mind the above mentioned features (for detailed discussion, see ref. 75).

An entirely new catalytic site containing manganese as redox active transition metal centres is required for performing oxidative water splitting. This water oxidizing complex (WOC) is unique among all photosynthesizing organisms (for an updated review on PS II, see ref. 77). Interestingly, the basic functional pattern of the WOC remained virtually invariant to evolutionary development from early oxygen evolving cyanobacteria up to the level of higher plants⁷⁸.

Significant progress has been made in unravelling the structure of PS II at atomic resolution and the currently most advanced level reached is at 2.9 Å (ref. 79). The top panel of Figure 7 shows the overall structure of the core complex (Figure 7a) and the arrangement of the cofactors (Figure 7b). All cofactors are bound to a heterodimeric protein matrix consisting of polypeptides D1 and D2. A comparison of this array with the top panel of Figure 5 reveals that the folding pattern of D1 and D2, each forming five transmembrane helices, and the array of the four central Chl *a* molecules, the two Pheos, the two quinones Q_A and Q_B and the non heme (NH) Fe are similar to the structure of the L/M heterodimer and the arrangement of the corresponding BChls, BPheos, Q_A, Q_B and NHFe in RCs from anoxygenic purple bacteria. The only striking structural difference is the presence of two additional Chl *a* molecules at the periphery and of the Mn₄O₄Ca cluster of the WOC in PS II. Furthermore, the axial ligand Glu of NHFe in photosynthetic bacterial (PB)RCs is replaced by carbonate in PS II (see ref. 82 and references therein). This change of the coordination is probably responsible for the well-established 'bicarbonate effect' on the acceptor side of PS II (for reviews, see refs 83 and 84) including differences in the pathways for protonation transfer to the Q_B site⁸⁵.

In marked contrast to the widely conserved structural arrangement of the D1/D2 heterodimer and the cofactors involved in the formation of P680⁺ Q_A[•], the evolution of PS II comprised a drastic change of the polypeptide pattern compared to type II RCs of anoxygenic bacteria. All PS II core complexes contain about 20 subunits⁸⁶ versus two or three of RCs^{6–8} and this characteristic pattern of PS II was only slightly changed during evolution⁸⁷. Most of these subunits are intrinsic proteins. Two pigment binding proteins (CP47 and CP43), each forming six transmembrane helices, are intimately bound to the D1/D2 heterodimer. These two proteins not only act as core antenna of PS II but are also indispensable for the assembly of the WOC. Furthermore, a cytochrome *b559* (Cyt *b559*) is tightly bound to the D1/D2 heterodimer as an intrinsic membrane protein. This component with unusual redox properties is probably involved in protection

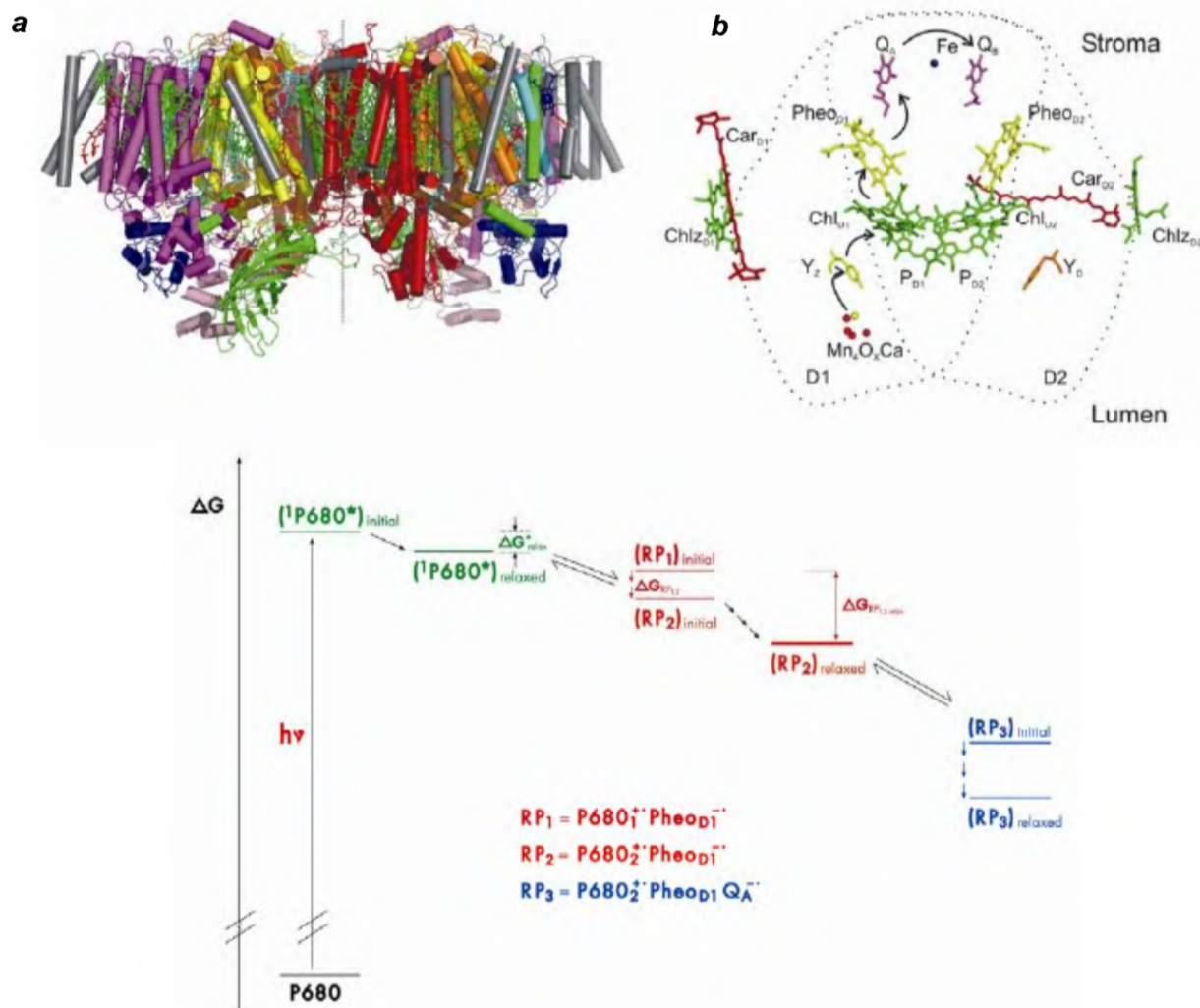


Figure 7. Top panel (provided by J. Kern): (a) A view along the membrane plane of a dimer of PS II from *T. elongatus* as derived from the 3.0 Å resolution electron density⁸⁰. (b) A schematic representation of the cofactor arrangement in the reaction centre core. Helices are depicted as cylinders, cofactors are drawn in stick models. The C2 axis, relating the two monomers in the dimer, is indicated by a black dashed line. The large subunits D1 (yellow) and D2 (orange), forming the reaction centre, are surrounded by CP43 (magenta) and CP47 (red) as well as several membrane intrinsic low molecular weight subunits (grey). The α and β subunits of the membrane intrinsic heterodimeric Cyt b559 are shown in green and cyan respectively. At the luminal side, the three extrinsic subunits PsbO (green), PsbV (blue) and PsbU (light pink) are known to interact with large loop regions of D1/D2/CP43/CP47. Organic cofactors are coloured in green (Chl), yellow (Pheo), magenta (PQ9), red (carotenoids), cyan (lipids) and blue (haeme) respectively, Ca²⁺ (yellow) Fe (blue) and Mn (red) are shown as spheres; the figure was generated using Pymol (Delano, 2003). (b) Cofactor arrangement in the PS II core (coloured as in a, view is along the membrane plane), the coordinating protein subunits D1 and D2 are indicated by a dotted line. The P680, as defined in this review, is most likely formed by the four Chl P_{D1}/P_{D2}/Chl_{D1}/Chl_{D2} and possibly the pair Pheo_{D1}/Pheo_{D2} (see text). Black arrows symbolize the direction of electron transfer following excitation of P680 (for further details, see ref. 81). Bottom panel: Simplified scheme of the energetics of P680⁺Q_A⁻ formation. Symbols denote: (P680*)_{initial} and (P680*)_{relaxed} = excited singlet state of P680 in the initial state and in relaxed environment; RP₁, RP₂ and RP₃ = radical pair states as indicated in the insert, indices 'initial' and 'relaxed' indicate the initial form and the species in the relaxed environment respectively (electronic version prepared by S. Renger). See text for details.

against photoinhibition^{88,89}. In addition to Cyt b559, other small intrinsic proteins (PsbH to PsbN, PsbT, PsbX, PsbY, PsbZ) are characterized by each lacking a cofactor and forming one transmembrane helix. The physiological relevance of this 'evolutionary jump' from type II RCs of anoxygenic photosynthesis to PS II is not yet known. It appears likely that this complex polypeptide composition

is required for the stabilization of the 'water splitting machine'.

At least three proteins are bound to the luminal side of the complex as extrinsic regulatory subunits. One of these (subunit PsbO) is a constituent of the PS II complex of all oxygen evolving organisms and essential for stabilizing the catalytic manganese cluster while the other subunits

were entirely changed during evolution from cyanobacteria to plants (see ref. 90 and references therein).

The reaction sequence of light induced charge separation in PS II, summarized in the bottom panel of Figure 7, shows that the formation of the radical pair $P_{RC}^{+\bullet} \text{Acc}_2^{-\bullet}$ comprises three steps (for details, see ref. 75): (i) charge separation leading from the lowest excited singlet state $^1\text{Chl}_{D1}^*$ to the primary radical ion pair $\text{Chl}_{D1}^{+\bullet}\text{Pheo}_{D1}^{-\bullet}$, (ii) rapid reduction of $\text{Chl}_{D1}^{+\bullet}$ by $P_{D1}-P_{D2}$, where the spin in the radical $(P_{D1}-P_{D2})^{+\bullet}$ is predominantly located on $P_{D1}^{+\bullet}$ in intact PS II with a functionally competent WOC but after a severe modification a significant spin distribution emerges between P_{D1} and P_{D2} concomitant with a drop of the E_m value⁹¹ and (iii) stabilization of the radical pair formation by ET from $\text{Pheo}_{D1}^{-\bullet}$ to Q_A . The rate constant of the first step is still a matter of controversy because direct measurements are difficult due to the spectral overlap of the six coupled pigments forming the $\text{Chl } a_4 \text{ Pheo } a_2$ complex (for details, see refs 50 and 75 and references therein). On the other hand, the reoxidation kinetics of $\text{Pheo}_{D1}^{-\bullet}$ by Q_A were directly measured by time resolved absorption changes reflecting $\text{Pheo}_{D1}^{-\bullet}$ reoxidation⁹² and concomitant Q_A reduction⁹³.

The formation of $P680^{+\bullet} Q_A^{-\bullet}$ takes place down to liquid helium temperatures⁹⁴, whereas the reoxidation of $Q_A^{-\bullet}$ by $Q_B/Q_B^{-\bullet}$ at the Q_B site exhibits a striking dependence on temperature and hydration level^{95,96}. This finding shows that the protein flexibility affects the reaction pattern of type II RCs virtually in the same manner in both anoxygenic PBRCs and oxygenic PS II. The reactions of the WOC exhibit analogous effects (for a review, see ref. 97 and references therein).

The reaction sequence readily reveals a marked difference between the type II RCs in anoxygenic bacteria and PS II with respect to the function of the cofactors BChl_A and Chl_{D1} . In PBRCs, the monomeric BChl_A (see Figure 5 b, top panel) acts as an electron acceptor in the primary charge separation step leading to the formation of $P^{+\bullet} \text{BChl}_A^{-\bullet}$, whereas in PS II the Chl_{D1} (see Figure 7 b, top panel) in its lowest excited singlet state is the electron donor for the formation of the primary radical pair $\text{Chl}_{D1}^{+\bullet} \text{Pheo}_{D1}^{-\bullet}$ (for further details, see ref. 75). The feature of PS II basically resembles that of PS I (see the previous section). It is most interesting to note that the role of the 'special pair' and direction of the primary charge separation step have been significantly changed in the evolutionary transition from anoxygenic to oxygenic photosynthesis. The physiological reason for this change is not yet known and remains a challenging task for future research.

The fraction of the energy of a 680 nm photon, transiently stored in the radical pair $P680^{+\bullet} Q_A^{-\bullet}$ (the spin of $P680^{+\bullet}$ is mainly localized on P_{D1} , see ref. 91), is estimated to be about 70% when using E_m -values of +1.25 V of $P680/P680^{+\bullet}$ and about -0.1 V for $Q_A^{-\bullet}/Q_A$ (for a review, see ref. 75). Compared to type II RCs of anoxygenic bacteria (see section on 'Reaction centres of ano-

xygenic purple bacteria'), this fraction of transiently stored Gibbs free energy is higher by a factor of about two. This marked increase is entirely due to the drastically enhanced redox potential of $P680$ compared to P .

Conclusions

Photosynthetic RCs are the solar batteries of life that transform the electromagnetic radiation from the Sun into electrochemical Gibbs free energy fluxes. In non-oxygen evolving organisms (anoxygenic bacteria), RCs are autonomous units consisting of two or three polypeptides and the cofactors for light induced 'stable' charge separation. They are characterized by a quantum yield of close to one for radical pair formation and are functionally connected with light harvesting antenna systems and ET components. Two types of RCs exist. Anoxygenic photosynthetic bacteria contain only one type of RC which energetically drives the electron transport chain and phosphorylation. The 'big bang' in evolution was the invention of oxygen evolving organisms, where the transformation of type II RC into a 'water-spitting machine' was the cornerstone. This evolution was accompanied by integration of RCs into larger complexes referred to as photosystem I and II and by functional connection of these complexes to form an electron transport chain for water splitting into molecular dioxygen and hydrogen chemically bound to NADP^+ .

Reaction centres and photosystems are masterpieces for efficient solar energy exploitation by nanoscale machines and therefore offer most suitable 'blueprints' for designing technical devices to satisfy mankind's increasing Gibbs free energy demand without the risk of a global climate disaster.

1. Boltzmann, L., Der zweite Hauptsatz der Wärmetheorie. In *Populäre Schriften*, J. A. Barth, Leipzig (in German), 1884.
2. Morowitz, H. J., *Foundations of Bioenergetics*, Academic Press, New York, 1978.
3. Nicolis, G. and Prigogine, I., *Self Organization in Nonequilibrium Systems*, Wiley, New York, 1977.
4. Zamaraev, K. I. and Parmon, V. N., Potential methods and perspectives of solar energy conversion via photocatalytic processes. *Rev. Sci. Eng.*, 1980, **22**, 261–324.
5. van Niel, C. B., The bacterial photosynthesis and their importance of the general problem of photosynthesis. *Act. Enzymol.*, 1941, **1**, 263–328.
6. Blankenship, R. E., Madigan, M. T. and Bauer, C. E. (eds), *Anoxygenic Photosynthetic Bacteria, Advances in Photosynthesis and Respiration* (Series ed. Govindjee), Kluwer, Dordrecht, 1995, vol. 2.
7. Parson, W. W., Functional pattern of reaction centers in anoxygenic photosynthetic bacteria. In *Primary Processes of Photosynthesis: Principles and Apparatus, Part II, Reaction Centers/Photosystems, Electron Transport Chains, Photophosphorylation and Evolution* (ed. Renger, G.), Royal Society Chemistry, Cambridge, 2008, pp. 57–109.
8. Hunter, C. N., Daldal, F., Thurnauer, M. C. and Beatty, J. T. (eds), *The Purple Phototrophic Bacteria: Advances in Photosynthesis*

- and Respiration (Series ed. Govindjee), Springer, Dordrecht, 2009, vol. 28.
9. Kasting, J. F. and Seifert, J. F., Life and the evolution of earth's atmosphere. *Science*, 2002, **296**, 1066–1067.
 10. Lane, N., *Oxygen – The Molecule that Made the World*, Oxford University Press, Oxford, 2003.
 11. Larkum, A. W. D., The evolution of photosynthesis. In *Primary Processes of Photosynthesis: Principles and Apparatus, Part II, Reaction Centers/Photosystems, Electron Transport Chains, Photophosphorylation and Evolution* (ed. Renger, G.), Royal Society of Chemistry, Cambridge, 2008, pp. 491–521.
 12. Ke, B., *Photosynthesis – Photobiochemistry and Photobiophysics, Advances in Photosynthesis and Respiration* (Series ed. Govindjee), Kluwer, Dordrecht, 2001, vol. 10.
 13. Björn, L. O. and Govindjee, The evolution of photosynthesis and chloroplasts. *Curr. Sci.*, 2009, **96**, 1466–1474.
 14. Scheer, H., Chlorophylls. In *Primary Processes of Photosynthesis: Principles and Apparatus, Part I, Photophysical Principles, Pigments and Light Harvesting/Adaptation/Stress* (ed. Renger, G.), Royal Society Chemistry, Cambridge, 2008, pp. 101–149.
 15. Polivka, T. and Sundström, V., Ultrafast dynamics of carotenoid excited states – from solution to natural and artificial systems. *Chem. Rev.*, 2004, **104**, 2021–2072.
 16. Emerson, R. and Arnold, W., The photochemical reaction in photosynthesis. *J. Gen. Physiol.*, 1932, **16**, 191–205.
 17. Gaffron, H. and Wohl, K., On the theory of assimilation. *Naturwissenschaften*, 1936, **24**, 81–90.
 18. Renger, G., Molecular mechanism of water oxidation. In *Concepts in Photobiology: Photosynthesis and Photomorphogenesis* (eds Singhal, G. S. et al.), Kluwer, Dordrecht and Narosa Publishing, Delhi, 1999, pp. 292–329.
 19. Pearlstein, R. M., Chlorophyll singlet exciton. In *Photosynthesis I, Energy Conversion by Plants and Bacteria* (ed. Govindjee), Academic Press, New York, 1982, pp. 293–330.
 20. Renger, T., Theory of excitation energy transfer: from structure to function. *Photosynth. Res.*, 2009, **102**, 471–485.
 21. Renger, T., Absorption of light, excitation energy transfer and electron transfer reactions. In *Primary Processes of Photosynthesis: Principles and Apparatus, Part I, Photophysical Principles, Pigments and Light Harvesting/Adaptation/Stress* (ed. Renger, G.), Royal Society Chemistry, Cambridge, 2008, pp. 39–97.
 22. Förster, T., Delocalized excitation and excitation transfer. In *Modern Quantum Chemistry* (ed. Sinnanoglu, O.), Academic Press, New York, 1965, pp. 257–265.
 23. Lakowicz, J. R., *Principles of Fluorescence Spectroscopy*, Kluwer, New York, 1999, 2nd edn.
 24. Dexter, D. L., A theory of sensitized luminescence in solids. *J. Chem. Phys.*, 1953, **21**, 836–850.
 25. Renger, G., Energy transfer and trapping in photosystem II. In *Topics in Photosynthesis, the Photosystems: Structure, Function and Molecular Biology* (ed. Barber, J.), Kluwer, Dordrecht, 1992, pp. 45–99.
 26. Siefertmann-Harms, D., The light-harvesting and protective functions of carotenoids in photosynthetic membranes. *Physiol. Plant.*, 1987, **69**, 561–568.
 27. Schödel, R., Irrgang, K.-D., Voigt, J. and Renger, G., Rate of carotenoid triplet formation in solubilized light-harvesting complex II (LHCII) from spinach. *Biophys. J.*, 1998, **75**, 3143–3153.
 28. Clegg, R. M., Sener, M. and Govindjee, From Förster resonance energy transfer to coherent resonance energy transfer and back. In *Optical Biophysics VII, Proceedings of SPIE* (ed. Alfano, R. R.), SPIE, Bellingham, WA, 2010, vol. 7561.
 29. De Vault, D., *Quantum-mechanical Tunneling in Biological Systems*, Cambridge University Press, Cambridge, 1984, 2nd edn.
 30. Marcus, R. A. and Sutin, N., Electron transport in chemistry and biology. *Biochim. Biophys. Acta*, 1985, **811**, 265–322.
 31. Moser, C. C., Keske, J. M., Warneke, K., Farid, R. S. and Dutton, P. L., Nature of biological electron-transfer. *Nature*, 1992, **355**, 796–802.
 32. Moser, C. C., Farid, T. A., Chobot, S. E. and Dutton, P. L., Electron tunneling chains of mitochondria. *Biochim. Biophys. Acta*, 2006, **1757**, 1096–1109.
 33. Gray, H. B. and Winkler, J. R., Electron transfer in proteins. *Annu. Rev. Biochem.*, 1996, **65**, 537–561.
 34. Atkins, P. W., *Physical Chemistry*, Oxford University Press, Oxford, 2001.
 35. Duysens, L. M. N., The path of light energy in photosynthesis. *Brookhaven Symp. Biol.*, 1959, **11**, 10–25.
 36. Knox, R. S., Photosynthetic efficiency and exciton transfer and trapping. In *Primary Processes of Photosynthesis* (ed. Barber, J.), Elsevier, Amsterdam, 1977, pp. 55–97.
 37. Milo, R., What governs the reaction center excitation wavelength of photosystems I and II? *Photosynth. Res.*, 2009, **101**, 59–67.
 38. Bell, L. N. and Gudkov, N. D., Thermodynamics of light energy conversion. In *Topics in Photosynthesis, the Photosystems: Structure, Function and Molecular Biology* (ed. Barber, J.), Elsevier, Amsterdam, 1992, pp. 17–43.
 39. Almgren, M., Thermodynamic and kinetic limitations of the conversion of solar energy into storable chemical free energy. *Photochem. Photobiol.*, 1978, **27**, 603–609.
 40. Jennings, R. C., Engelmann, E., Garlaschi, F., Casazza, A. P. and Zucchelli, G., Photosynthesis and negative entropy production. *Biochim. Biophys. Acta*, 2005, **1709**, 251–255.
 41. Knox, R. S. and Parson, W. W., Entropy production and the Second Law in photosynthesis. *Biochim. Biophys. Acta*, 2007, **1767**, 1189–1193.
 42. Parson, W. W., Thermodynamics of the primary reactions in photosynthesis. *Photochem. Photobiol.*, 1978, **28**, 389–393.
 43. Law, C. J. and Cogdell, R. J., The light-harvesting system of purple anoxygenic photosynthetic bacteria. In *Primary Processes of Photosynthesis: Principles and Apparatus, Part I, Photophysical Principles, Pigments and Light Harvesting/Adaptation/Stress* (ed. Renger, G.), Royal Society of Chemistry, Cambridge, 2008, pp. 205–259.
 44. Green, B. and Parson, W. W. (eds), *Light Harvesting Antennas. Advances in Photosynthesis and Respiration*, Springer, Dordrecht, 2003, vol. 13.
 45. Renger, G. (ed.), *Primary Processes of Photosynthesis: Principles and Apparatus, Part I, Photophysical Principles, Pigments and Light Harvesting/Adaptation/Stress*, Royal Society of Chemistry, Cambridge, 2008.
 46. Reed, D. W. and Clayton, R. K., Isolation of a reaction center fraction from *Rhodospseudomonas spheroides*. *Biochem. Biophys. Res. Commun.*, 1968, **30**, 471–475.
 47. Clayton, R. K., Research on photosynthetic reaction centers from 1932–1987. In *Discoveries in Photosynthesis. Advances in Photosynthesis and Respiration* (eds Govindjee et al.), Springer, Dordrecht, 2005, vol. 20, pp. 195–203.
 48. Liebl, U., Mockensturm-Wilson, M., Trost, J. T., Brune, D. C., Blankenship, R. E. and Vermaas, W., Single core polypeptide in the reaction center of the photosynthetic bacterium *Helicobacillus mobilis*: structural implications and relations to other photosystems. *Proc. Natl Acad. Sci. USA*, 1993, **90**, 7124–7128.
 49. Wraight, C. A. and Clayton, R. K., The absolute quantum efficiency of bacteriochlorophyll photooxidation in reaction centres of *Rhodospseudomonas spheroides*. *Biochim. Biophys. Acta*, 1974, **333**, 246–260.
 50. Renger, G. and Holzwarth, A. R., Primary electron transfer. In *Photosystem II: The Water: Plastoquinone Oxido-reductase in Photosynthesis* (eds Wydrzynski, T. and Satoh, K.), Springer, Dordrecht, 2005, pp. 139–175.
 51. Crofts, A. R. and Wraight, C. A., The electrochemical domain of photosynthesis. *Biochim. Biophys. Acta*, 1983, **726**, 149–185.

52. Deisenhofer, J., Epp, O., Miki, K., Huber, R. and Michel, H., Structure of the protein subunits in the photosynthetic reaction centre of *Rhodospseudomonas viridis* at 3 Å resolution. *Nature*, 1985, **318**, 618–624.
53. Lancaster, R., Structures of reaction centers in anoxygenic bacteria. In *Primary Processes of Photosynthesis: Principles and Apparatus, Part II, Reaction Centers/Photosystems, Electron Transport Chains, Photophosphorylation and Evolution* (ed. Renger, G.), Royal Society of Chemistry, Cambridge, 2008, pp. 5–56.
54. Kirmaier, C., Cua, A., He, C. Y., Holten, D. and Bocian, D. F., Probing M-branch electron transfer and cofactor environment in the bacterial photosynthetic reaction center by addition of a hydrogen bond to the M-side bacteriopheophytin. *J. Phys. Chem. B*, 2002, **106**, 495–503.
55. Zinth, W. and Wachtveitl, J., The first picoseconds in bacterial photosynthesis – ultrafast electron transfer for the efficient conversion of light energy. *Chem. Phys. Chem.*, 2005, **6**, 871–880.
56. Schenck, C. C., Parson, W. W., Holten, D., Windsor, M. W. and Sarai, A., Temperature dependence of electron transfer between bacteriopheophytin and ubiquinone in protonated and deuterated reaction centers of *Rhodospseudomonas sphaeroides*. *Biophys. J.*, 1981, **36**, 479–489.
57. Graige, M. S., Feher, G. and Okamura, M. Y., Conformational gating of the electron transfer reaction $Q_A \rightarrow Q_B \rightarrow Q_A Q_B^{\bullet -}$ in bacterial reaction centers of *Rhodobacter sphaeroides* determined by a driving force assay. *Proc. Natl Acad. Sci. USA*, 1998, **95**, 11679–11684.
58. Heinen, U., Utschig, L. M., Poluektov, O. G., Link, G., Ohmes, E. and Kothe, G., Structure of the charge separated state $P_{680}^+ Q_A^-$ in the photosynthetic reaction centers of *Rhodobacter sphaeroides* by quantum beat oscillations and high-field electron paramagnetic resonance: evidence for light-induced Q_A^- reorientation. *J. Am. Chem. Soc.*, 2007, **129**, 15935–15946.
59. Golbeck, J. H. (ed.), *Photosystem I: The Light-induced Plastocyanin : Ferredoxin Oxidoreductase, Advances in Photosynthesis and Respiration* (Series ed. Govindjee), Springer, Dordrecht, 2006, vol. 24.
60. Jordan, P., Fromme, P., Klukas, O., Witt, H. T., Saenger, W. and Krauß, N., Three dimensional structure of cyanobacterial photosystem I at 2.5 Å resolution. *Nature*, 2001, **411**, 909–917.
61. Amunts, A., Drory, O. and Nelson, N., The structure of a plant photosystem I supercomplex at 3.4 Å resolution. *Nature*, 2007, **447**, 58–63.
62. Fromme, P. and Grotjohann, I., Structural analysis of cyanobacterial photosystem I. In *Photosystem I: The Light-induced Plastocyanin : Ferredoxin Oxidoreductase* (ed. Golbeck, J. H.), Springer, Dordrecht, 2006, pp. 47–69.
63. Kok, B., Absorption changes induced by the photochemical reaction of photosynthesis. *Nature*, 1957, **179**, 583–584.
64. Sétif, P. and Leibl, W., Functional pattern of photosystem I in oxygen evolving organisms. In *Primary Processes of Photosynthesis: Principles and Apparatus, Part II, Reaction Centers/Photosystems, Electron Transport Chains, Photophosphorylation and Evolution* (ed. Renger, G.), Royal Society of Chemistry, Cambridge, 2008, pp. 147–191.
65. van der Est, A., Electron transfer involving phyloquinones in photosystem I. In *Photosystem I: The Light-induced Plastocyanin : Ferredoxin Oxidoreductase* (ed. Golbeck, J. H.), Springer, Dordrecht, 2006, pp. 387–411.
66. Redding, K. and van der Est, A., The directionality of electron transport in photosystem I. In *Photosystem I: The Light-induced Plastocyanin : Ferredoxin Oxidoreductase* (ed. Golbeck, J. H.), Springer, Dordrecht, 2006, pp. 420–441.
67. Müller, M. G., Niklas, J., Lubitz, W. and Holzwarth, A. R., Ultrafast transient absorption studies on photosystem I reaction centers from *Chlamydomonas reinhardtii*. 1. A new interpretation of the energy trapping and early electron transfer steps in photosystem I. *Biophys. J.*, 2003, **85**, 3899–3922.
68. Giera, W., Ramesh, V. M., Webber, A. N., van Stokkum, I., van Grondelle, R. and Gibasiewicz, K., Effect of the P700 pre-oxidation and point mutations near A_0 on the reversibility of the primary charge separation in photosystem I from *Chlamydomonas reinhardtii*. *Biochim. Biophys. Acta*, 2010, **1797**, 106–112.
69. Shinkarev, V. P., Vassiliev, I. R. and Golbeck, J. H., A kinetic assessment of the sequence of electron transfer from F_X to F_A and further to F_B in photosystem I: the value of the equilibrium constant between F_X and F_A . *Biophys. J.*, 2000, **78**, 363–372.
70. Wydrzynski, T. and Satoh, K. (eds), *Photosystem II: The Water : Plastoquinone Oxido-reductase in Photosynthesis, Advances in Photosynthesis and Respiration* (Series ed. Govindjee), Springer, Dordrecht, 2005, vol. 22.
71. Hasegawa, K. and Noguchi, T., Density functional theory calculations on the dielectric-constant dependence of the oxidation potential of chlorophyll: implication for the high potential of P680 in photosystem II. *Biochemistry*, 2005, **44**, 8865–8872.
72. Ishikita, H., Saenger, W., Biesiadka, J., Loll, B. and Knapp, E. W., How photosynthetic reaction centers control oxidation power in chlorophyll pairs P680, P700, and P870. *Proc. Natl Acad. Sci. USA*, 2006, **103**, 9855–9860.
73. Kobayashi, M., Ohashi, S., Iwamoto, K., Shiraiwa, Y., Kato, Y. and Watanabe, T., Redox potential of chlorophyll *d* in vitro. *Biochim. Biophys. Acta*, 2007, **1767**, 596–602.
74. Rappaport, F. and Diner, B. A., Primary photochemistry and energetics leading to the oxidation of the (Mn)₄Ca cluster and to the evolution of molecular oxygen in photosystem II. *Coord. Chem. Rev.*, 2009, **252**, 259–272.
75. Renger, G. and Renger, T., Photosystem II: the machinery of photosynthetic water splitting. *Photosynth. Res.*, 2008, **98**, 53–80.
76. Renger, G. (ed.), Functional pattern of photosystem II. In *Primary Processes of Photosynthesis: Basic Principles and Apparatus, Reaction Centers/Photosystems, Electron Transport Chains, Photophosphorylation and Evolution*, Royal Society of Chemistry, Cambridge, 2008, vol. II, pp. 237–290.
77. Govindjee, K., Kern, J. F., Messinger, J. and Whitmarsh, J., Photosystem II. In *Encyclopedia of Life Sciences (ELS)*, John Wiley, Chichester, 2010; DOI: 10.1002/9780470015902.a0000669.pub2.
78. Renger, G., Photosynthetic water oxidation to molecular oxygen: apparatus and mechanism. *Biochim. Biophys. Acta*, 2001, **1503**, 210–228.
79. Guskov, A., Kern, J., Gabdulkhakov, A., Broser, M., Zouni, A. and Saenger, W., Cyanobacterial photosystem II at 2.9 Å resolution and the role of quinones, lipids, channels and chloride. *Nature Struct. Mol. Biol.*, 2009, **16**, 334–342.
80. Loll, B., Kern, J., Saenger, W., Zouni, A. and Biesiadka, J., Towards complete cofactor arrangement in the 3.0 Å resolution structure of photosystem II. *Nature*, 2005, **438**, 1040–1044.
81. Kern, J. and Renger, G., Photosystem II: structure and mechanism of the water : plastoquinone oxidoreductase. *Photosynth. Res.*, 2007, **94**, 183–202.
82. Cox, N., Jin, L., Jaszewski, A., Smith, P. J., Krausz, E., Rutherford, A. W. and Pace, R., The semiquinone-iron complex of photosystem II: structural insights from ESR and theoretical simulation; evidence that the native ligand to the non-heme iron is carbonate. *Biophys. J.*, 2009, **97**, 2024–2033.
83. Govindjee and van Rensen, J. J. S., Photosystem II reaction centers and bicarbonate. In *Photosynthetic Reaction Centers* (eds Deisenhofer, J. and Norris, J. R.), Academic Press, Orlando, 1993, vol. I, pp. 357–389.
84. van Rensen, J. J. S., Xu, C. and Govindjee, Role of bicarbonate in photosystem II, the water-plastoquinone oxido-reductase of plant photosynthesis. *Physiol. Plant.*, 1999, **105**, 585–592.
85. Suzuki, H., Nagasaka, M., Sugiura, M. and Noguchi, T., Fourier transform infrared spectrum of the secondary quinone electron

- acceptor Q(B) in photosystem II. *Biochemistry*, 2005, **44**, 11323–11328.
86. Shi, L.-X. and Schröder, W. P., The low molecular mass subunits of the photosynthetic supracomplex, photosystem II. *Biochim. Biophys. Acta*, 2004, **1608**, 75–96.
 87. Raymond, J. and Blankenship, R. E., The evolutionary development of the protein complement of photosystem 2. *Biochim. Biophys. Acta*, 2004, **1655**, 133–139.
 88. Stewart, D. H. and Brudvig, G. W., Cytochrome b_{559} of photosystem II. *Biochim. Biophys. Acta*, 1998, **1367**, 63–87.
 89. Kaminskaya, O., Shuvalov, V. A. and Renger, G., Evidence for a novel quinine binding site in the PS II (PS II) complex which regulates the redox potential of Cyt b_{559} . *Biochemistry*, 2007, **46**, 1091–1105.
 90. Enami, I., Okumura, A., Nagao, R., Suzuki, T., Iwai, M. and Shen, J. R., Structures and functions of the extrinsic proteins of photosystem II from different species. *Photosynth. Res.*, 2008, **98**, 349–363.
 91. Okubo, T., Tomo, T., Sugiura, M. and Noguchi, T., Perturbation of the structure of P680 and the charge distribution on its radical cation in isolated reaction center complexes of photosystem II as revealed by Fourier transform infrared spectroscopy. *Biochemistry*, 2007, **46**, 4390–4397.
 92. Bernarding, J., Eckert, H.-J., Eichler, H.-J., Napiwotzki, A. and Renger, G., Kinetic studies on the stabilization of the primary radical pair $P680^+Pheo^-$ in different photosystem II preparations from higher plants. *Photochem. Photobiol.*, 1994, **59**, 566–573.
 93. Groot, M. L., Pawlowicz, N. P., Van Wilderen, L. J. G. W., Breton, J., Van Stokkum, I. H. M. and van Grondelle, R., Initial electron donor and acceptor in isolated photosystem II reaction centers identified with femtosecond mid-IR spectroscopy. *Proc. Natl Acad. Sci. USA*, 2005, **102**, 13087–13092.
 94. Hughes, J. L., Smith, P., Pace, R. and Krausz, E., Charge separation in photosystem II core complexes induced by 690–730 nm excitation at 1.7 K. *Biochim. Biophys. Acta*, 2006, **1757**, 841–851.
 95. Renger, G., Gleiter, H. M., Haag, E. and Reifarth, F., Photosystem II: thermodynamics and kinetics of electron transport from Q_A^* to Q_B (Q_B^+) and deleterious effects of copper (II). *Z. Naturforsch.*, 1993, **48c**, 234–240.
 96. Kaminskaya, O., Renger, G. and Shuvalov, V. A., Effect of dehydration on light induced reactions in photosystem II: photoreactions of cytochrome b_{559} . *Biochemistry*, 2003, **42**, 8119–8132.
 97. Messinger, J. and Renger, G., Photosynthetic water splitting. In *Primary Processes of Photosynthesis: Basic Principles and Apparatus, Reaction Centers/Photosystems, Electron Transport Chains, Photophosphorylation and Evolution* (ed. Renger, G.), Royal Society of Chemistry, Cambridge, 2008, vol. II, pp. 291–349.

ACKNOWLEDGEMENTS. I have many people to thank: Frank Müh for critical reading and valuable comments, Govindjee for editing the manuscript, George Papageorgiou and two editors for helpful suggestions, Richard Cogdell, Petra Fromme, Ingo Grotjohann, Jan Kern, Bill Parson, Susanne Renger, Pierre Setif and Christoph Theiss for the electronic figures. The financial support by Deutsche Forschungsgemeinschaft (Sfb 429, TPA1) is gratefully acknowledged.

Received 12 March 2010; accepted 22 March 2010